IEEE Access
Multidisciplinary : Rapid Review : Open Access Journal

Received 10 February 2023, accepted 16 March 2023, date of publication 24 March 2023, date of current version 30 March 2023.
Digital Object Identifier 10.1109/ACCESS.2023.3261803

APPLIED RESEARCH

Demonstrating Intra-Spacecraft Optical Wireless Links

GIULIO COSSU[1], LORENZO GILLI[1], NICOLA VINCENTI[1], EMILIANO PIFFERI[2], VINCENZO SCHENA[2], AND ERNESTO CIARAMELLA[1], (Senior Member, IEEE)
[1]Scuola Superiore Sant'Anna, TeCIP Institute, 56127 Pisa, Italy
[2]Thales Alenia Space, 00131 Rome, Italy

Corresponding author: Giulio Cossu (g.cossu@santannapisa.it)

This work was supported by the European Space Agency (ESA) Project Transmission of Optical Wireless Signals for telecom satellites (TOWS) under Contract 4000125458/18/UK/NR.

ABSTRACT In a Spacecraft (SC), a huge amount of cabled electrical connections is needed by many different units to exchange digital data. This increases the overall mass, the space occupancy, and the routing design time. Here, we propose and demonstrate an Optical Wireless Communication (OWC) system that can perfectly replace the MIL-STD-1553B cables inside the SC, providing wireless communication among the satellite units, with full backward compatibility with pre-existing units and protocols. We present the experimental demonstration in the challenging environment of a populated mockup of a real SC, where we connect four different units and exploit the Non Line-of-Sight (NLOS) configuration, i.e. take advantage of the scattering from the walls to overcome the shadowing effects. This OWC technique can effectively reduce the overall weight (more than 50%) and cost of the SC data network. The proposed transceivers are based on a transparent, fully analog solution and are made of Commercial Off-the-Shelf (COTS) components, with features compatible with the space environment. The on-field experiment shows that this is a practical solution for the data networks in future SCs.

INDEX TERMS Optical wireless communication, spacecraft communication, airspace communication.

I. INTRODUCTION

Currently, a key problem in the design and realization of Spacecrafts (SCs) is due to the huge amount of data wires. Not only the harness of the cables represents a significant percentage of its mass (up to 8% [1]), it also poses relevant issues during the Assembly Integration and Test (AIT) phase [2]. In addition, the wired network suffers from other drawbacks: it requires time and cost for routing, placing and shielding the cables [1], [3].

Wireless communications can significantly reduce this electrical harness [4], [5], [6], [7]. Radio Frequency (RF) technologies, which were considered initially [6], introduce strong constraints in terms of Electro-Magnetic Compatibility (EMC) and security. Moreover, in order to have directional beams, arrays of antennas would be required [8].

Recently, the interest in Optical Wireless Communications (OWCs) is growing, as it is now considered an attractive complementary solution to RF, thanks to the high maturity reached by this technology [9]. OWC systems exploit wavelengths in the optical spectrum (visible or infrared) to transmit wireless; they thus provide no Electro-Magnetic Interference (EMI) and resistance to jamming/sniffing, significantly increasing the reliability and the security of the communication. OWC relies on different optical sources and detectors that allow to design specific systems that are strictly application-oriented, according to data-rate and coverage area: the lower is the bit-rate, the higher is the robustness and the area covered. Previous terrestrial research demonstrated two main classes of OWC links, that are the Directed Line-of-Sight (DLOS) links, with narrow beams, [10], [11] and the Non Line-of-Sight (NLOS) links, with wide beams [12], [13], [14], [15]. Clearly, DLOS systems have the highest transmission speed, whilst NLOS systems have the strongest robustness to shadowing and the widest coverage [14], [15]. Therefore the second ones are particularly suited for optical transmission in the environments that are rich of shadowing effects, such as the typical SC. Thanks to the recent

The associate editor coordinating the review of this manuscript and approving it for publication was Chan Hwang See.

developments, OWC technology, which had been considered for space application in past European Space Agency (ESA) programs [16], [17], [18], [19], is now experiencing a renovated interest.

In this framework, ESA funded the project Transmission of Optical Wireless Signals for telecom satellites (TOWS) to develop simple interfaces replacing cabled communications with free-space optical signals. To this aim, we proposed a novel approach, by seamless replacing the cables of the MIL-STD-1553B (communication standard widely used in SC [20], [21], [22]) with a pluggable OWC device able to transmit and receive the data wireless and transparently, having complete compatibility with the pre-existing equipment. Namely, the MIL-STD-1553B standard [23] defines a moderate speed (1 Mbit/s) digital time division command/response multiplexed data bus, which is suitable of NLOS communications; unfortunately, some of its key properties make it hard any direct use in OWC links.

In TOWS, we addressed these issues and considered three different challenging scenarios [24]: intra-SC, extra-SC and AIT. Each of them shows very different requirements and, therefore, different configurations may be required. Among the scenarios, the most attractive is the intra-SC, where different units regularly exchange digital data with the System Main Unit (SMU). This application scenario is the most challenging: the Line-of-Sight (LOS) between the Transmitter (TX) and Receiver (RX) is not guaranteed and usually is not possible, because the SC is populated by many different pieces of equipment, which produce shadows. Thus, an NLOS OWC system has to be designed and realized: this type of system is able to establish a connection by exploiting reflection/scattering from the various inner elements as well as from the walls of the SC. Clearly, any NLOS OWC system has much lower received power, thus can typically operate at much lower bit rate than the common LOS OWC systems.

Here, we present for the first time the application of our novel OWC transceivers in Intra-SC, which aim at replacing the MIL-STD-1553B cables. We report the experimental tests carried out within a populated mock-up of a real satellite (Cosmo-SkyMed), where the OWC transceivers were installed. We emulated a bus MIL-STD-1553B network connecting wirelessly four different units positioned in the most representative areas of the satellite.

The Manuscript is organized as follows. In Section II, we present the mock-up used for the experimental demonstration and we briefly describe the working principle of our OWC transceivers. In Section III, we report the transmission results, first about a single point-to-point link and then emulating a complete MIL-STD-1553B network, with all units actively connected. In Section IV, we report the optical characterization of the mock-up, which allows to determine the feasibility of communication when placing the transceivers should operate in other, different, positions. Finally, in Section V, we summarize the key results and draw the conclusion.

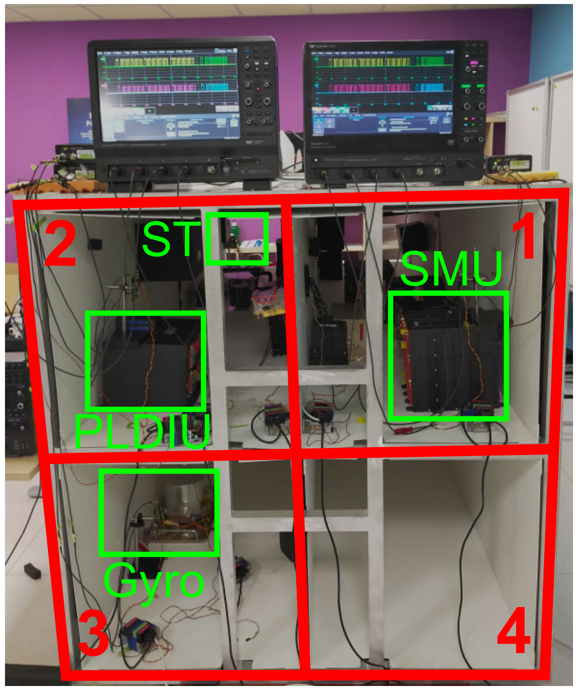

FIGURE 1. Front view of the Cosmo-SkyMed mock-up. Highlighted in green the positions of the connected devices inside the satellite rooms (red lines). SMU: System Main Unit; ST: Star Tracker; PLDIU: PayLoad Distribution Interface Unit; Gyro: Gyroscope. Oscilloscopes show real-time traces of detected packets. Close to the oscilloscopes, we can see the test modules. Here, the front panel was removed, but it was closed during all the measurements, so that we had no relevant background noise in the SC.

II. EXPERIMENTAL SETUP

A. MOCK-UP ARRANGEMENT

In order to perform the tests in a relevant environment, we could access the mock-up of the Cosmo-SkyMed satellite, available at Thales Alenia Space facilities, in Rome [25].

This mock-up is a parallelepiped with 120 cm length, 120 cm height and 316 cm depth. A picture is shown in Fig. 1: for clarity, the front panel was removed, as in most of the measurements. As we see, the cavity is divided in four identical rooms (highlighted and numbered in red), having both length and height equal to 60 cm. In our tests, the SMU is in room #1, for symmetry, room #2 and #4 are equivalent, thus we only placed our test units in room #1, #2 and #3. The relevant rooms were populated with dummy units that simulate the satellite onboard equipment and produce a realistic internal environment: the presence of these units is a key limiting factor to OWC transmission, as it can shadow the optical paths and interrupt the LOS of the links. Indeed, we design the OWC system to work in a NLOS architecture: the light from any TX illuminates all the corresponding room, so that it can always reach any RX in the same room, exploiting the scattering from the boxes and from inner walls. In this picture, the front panel was removed to show the internal set-up; however, during the tests the panel was practically closed, in order to emulate the real environment (a minor opening was left for the cables of the testing equipment).

Minor differences were found when operating the system with the panel off, because the room has only artificial lighting, which has a minor measurable component at the operation window (850 nm).

In the MIL-STD-1553B bus, all data links include the SMU, which acts as master, interrogating the various units and allocating the time slot for their replies. In our case, the position of the Transceiver (TRX) acting as Bus Controller (BC) corresponds to that of a SMU, we also selected the other units so that they are placed in the positions of PayLoad Distribution Interface Unit (PLDIU), Star Tracker (ST) and Gyroscope (Gyro) in the real SC. They all provide good representative examples of very different possible links, with disparate physical constrains. Therefore, we implemented the following links:

a) SMU–PLDIU link: the two units are located in two different cavities (rooms #1 and #2) separated by a single wall (as represented in Fig. 2a);
b) SMU–Gyro link: this is the most challenging case, since the Gyro is located in a cavity (room #3) diametrically opposed to the one of the SMU (see Fig. 2b);
c) SMU–ST link: ST is placed on the top floor of the SC in a position corresponding to the same cavity where the PLDIU is placed (room #2, see Fig. 2c); this is the longest link: its feasibility allows to reach via OWC an external unit, the ST, which is very far PLDIU, as it is located on the other side (roof) of the SC.

In all cases, the SMU unit works as BC and the other units as Remote Terminals (RTs), and all links are bidirectional, as specified by the MIL-STD-1553B standard [23]. We also outline that, although the signal at each RX can be due to various different contributions coming from different paths, we have no significant multipath impairment. Indeed, considering the satellite size, we can see that the delay introduced by the different light paths is in the order of tens of ns, i.e. it is much lower than the bit time (1 µs) so that we have no significant broadening of the transmitted bits. Furthermore, the emitter is a Light Emitting Diode (LED), hence it produces a lightwave signal that is incoherent; therefore we will never observe any type of interference.

It is obviously impossible to connect by means of optical signals three rooms that are perfectly isolated; indeed, in any real SC there are openings for cables, which might allow the light to pass. Here we had two openings $10 \times 10\,\text{cm}^2$: the first one was between rooms #1 and #2, and the second one was between rooms #2 and #3. The area of the openings was the maximum allowed by design in the inner walls of the SC. As a preliminary test, we measured the received optical power at the RTs units (PLDIU, ST and Gyro) using as light source the optical transmitter on the SMU. In this case, the link with SMU–PLDIU showed an acceptable power level, however, the measured optical power values were too low (<—40 dBm) for the SMU–ST and SMU–Gyro links. As a result, a reliable bus with all units was not possible. However, increasing the number of openings or widening them was not a viable solution. Therefore, we decided to realize and deploy two optical

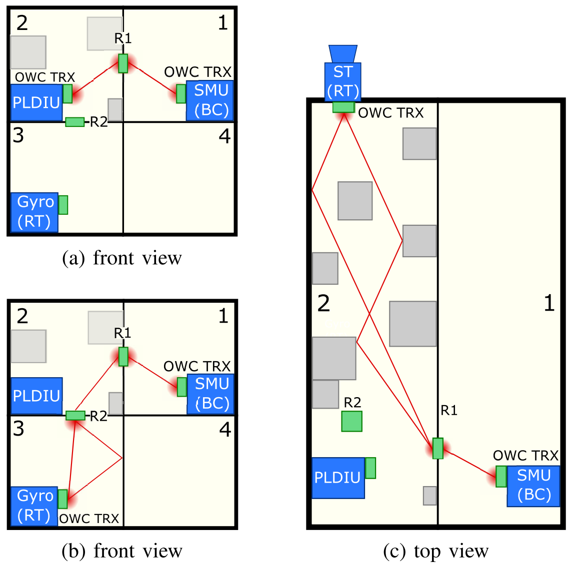

(a) front view

(b) front view

(c) top view

FIGURE 2. Scheme of the OWC links in the satellite. (a): SMU–PLDIU link; (b): SMU–Gyro link; (c): SMU–ST link. OWC boards are represented as green rectangles. Red lines indicate few possible light paths among the boards. Gray boxes denote the presence of dummy units, which can produce shadows. Rooms are labeled by the numbers.

signal regenerators (R1 and R2), each of them working as a range extender: R1 and R2 were placed on the openings between rooms #1 and #2 and rooms #2 and #3, respectively. The structure of the regenerators will be discussed in the following section.

B. TRANSCEIVERS AND REGENERATORS

Here, we briefly recall the key features of the OWC TRX [26] and introduce the regenerators. We designed a single TRX that can work in all different TOWS scenarios and provides optical wireless connectivity to the MIL-STD-1553B bus. The same TRX can work for all the different types of terminals of the bus (i.e., BC, RT and Bus Monitor (BM) [23]). This approach allows for high flexibility and high interoperability of the proposed solution. We also underline that no Digital Signal Processing (DSP) was used in these realizations, but only analogue Commercial Off-the-Shelf (COTS) devices, allowing for simple implementation and fast industrialization.

As shown in Fig. 3a, each TRX is composed by three functional parts [26]: the signal adaptation, the TX and the RX. The adaptation module converts the MIL-STD-1553B bipolar differential Manchester-encoded signal into an unipolar single-ended On-Off Keying (OOK) signal, and vice-versa. This is required to make the signal compatible with OWC transmission, e.g., the optical source does not allow a negative electrical input. Moreover, thanks to this approach, the optical source is active only during data transmission: this reduces the complexity of the electronics and significantly lessens the power consumption. In addition, the adaptation module recognizes the direction of the data flow, with no DSP, and is used to prevent the electronic crosstalk between TX and RX on the same TRX board.

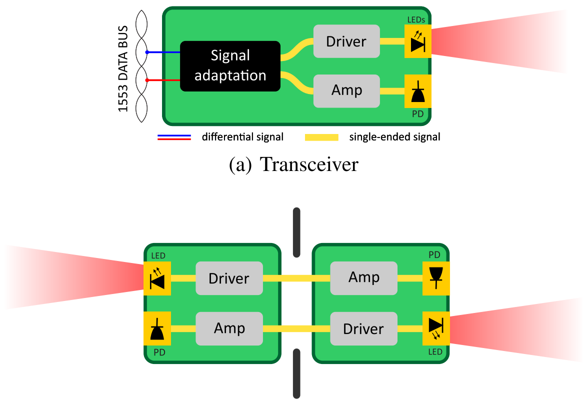

(a) Transceiver

(b) Regenerator

FIGURE 3. Schematic representation of the OWC transceiver (a) and of the regenerator (b).

The TX module includes the electronics to correctly modulate the optical source with the required optical power. Conveniently, the TRX operates at the wavelength of 850 nm, where both sources and detectors are widely available. It is designed to work in an optical NLOS configuration, leveraging on the wall/ceiling reflections: therefore, the light source is a Infrared (IR) LED, because it has wider emission angle (here around 150°) and higher optical power (here around 1 W) than a common laser diode.

The RX module is made by the Photo-Diodes (PDs), a Transimpedance Amplifier (TIA), a Low Pass Filter (LPF) and a comparator, which eventually performs threshold-decision and restores the required voltage levels. In order to minimize size, cost and power consumption, the PD is a PIN with about 25 mm^2 active area, 0.55 A/W responsivity at 850 nm, and ±65° Field-of-View (FoV). The large FoV is the second key feature of a NLOS TRX. We note that, in the RX board, we placed several test points that allow us to probe the signal at the different stages (e.g., after PD or after decision).

The three links described in Section II-A were established by four TRXs (one for each unit, shown Fig. 2). We also realized and used two regenerators (R1 and R2): each of them is made of two identical pairs of TXs and RXs, mounted back-to-back: the electrical signal from the first RX, after threshold-decision, is the electrical input to the second TX and vice-versa. We outline that in this case the boards only work with the OOK OWC signal, because it is not needed to convert it into/from a MIL-STD-1553B signal: each of the two parts can be viewed as a simplified version of the complete TRX (as shown in Fig. 3b). Each regenerator thus allows the correct signal coverage of two adjacent rooms, in both transmission directions: as the area of an acceptable opening cannot exceed the limit and shadowing effects are strong, each regenerator provides an adequate illumination level in the two rooms. This allows the required signal distribution in all rooms.

In summary, the same TX and RX modules show a very high flexibility, because they can be used in different contexts: when combined with the adaptation stage, they realize a TRX module that can be used with no limitation for all elements on the bus. Without the adaptation stage, the TX and RX can be also used to realize the OWC regenerator.

The used TRXs had limited weight (around 40 g) and low power consumption (around 0.5 W). This was a promising outcome, although no specific optimization had yet been performed: indeed, we expect that these figures can be further reduced in future implementations. The use of the wireless TRXs allows to strongly reduce the overall weight of the communication network. As an example, in the application scenario described in Section II-A, we estimate that if the cabled connections are replaced by OWC we can achieve a significant weight reduction (around 30% in the present configuration with 4 units, up to 60%, if we consider a complete bus with 32 RTs).

III. TRANSMISSION EXPERIMENTS

A. EXPERIMENTAL SETUP

The experimental setup of the MIL-STD-1553B network is schematically represented in Fig. 4: here we can see the four TRXs, the two repeaters and the walls. At each unit, the electrical MIL-STD-1553B signals were generated and received by means of one Test Module (TM) by Avionics Interface Technologies, which is the standard piece of equipment to test this type of signals. The four TMs emulate the behavior of all the different devices (BC, RTs and also the BM) active on the bus, initiating and monitoring all the communications among them. By using a Personal Computer (PC) connected to the TM, we can then extract the relevant information about the status of the connections. In particular, a home-made software routine on the PC reads the logbook of the TMs and converts the various words from the hexadecimal format into a binary format [26]: by analyzing the data streams at bit level, this allows us to monitor the communication performance of all the units on the bus and derive exact information about the status of the OWC-MIL-STD-1553B connections.

Before the test of the complete network, we performed a preliminary analysis and assessed the bidirectional communication of the three optical links, individually (i.e., point-to-point link). For the sake of simplicity, we will only report and describe one of the three links, i.e., the SMU–PLDIU link. This does not limit the generality of the description since the other point-to-point links showed similar results. Mostly, all links were eventually tested simultaneously working in the real MIL-STD-1553B bus network, where transmission was achieved thanks to the OWC system.

We indicate in dashed rectangular shape in Fig. 4 the parts involved in the experimental setup of the point-to-point transmissions between SMU–TRX and PLDIU–TRX. The electrical waveform was generated by the first TM (TM#1, working as BC) and fed to the SMU–TRX, which produces the optical signal. After free-space transmission, the optical signal was detected by the regenerator (R1) and optically re-transmitted in room #2, where it could be detected by the

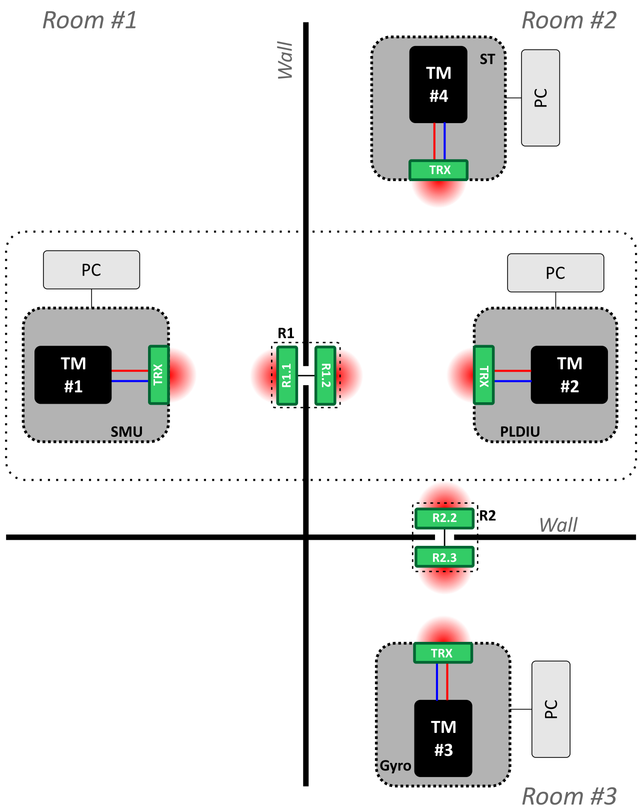

FIGURE 4. **Experimental setup of the MIL-STD-1553B network, including links among the four OWC units in three separate rooms. TM: Test Module; TRX: transceiver; PC: personal computer; R1, R2: regenerators.**

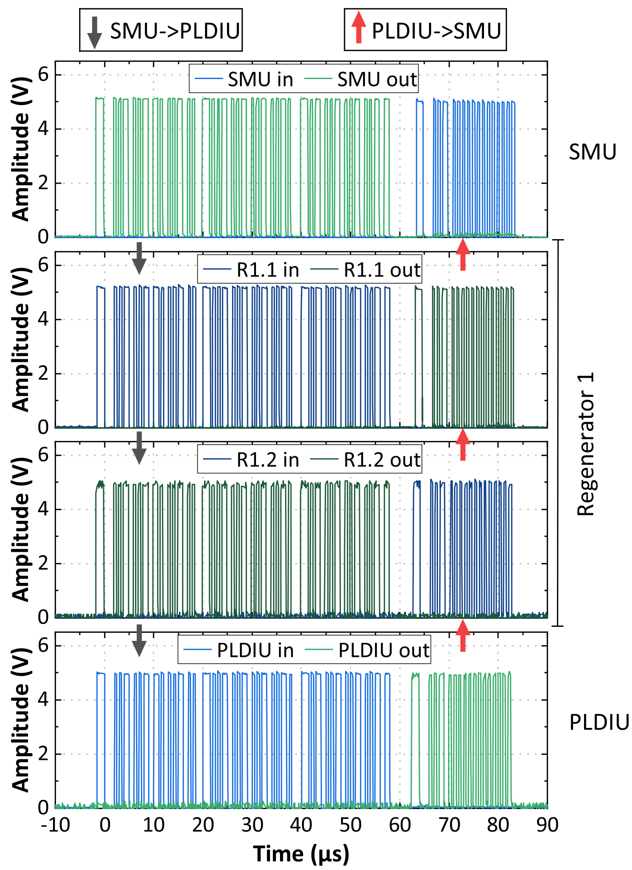

FIGURE 5. **Electrical signals taken at different points in the link SMU–PLDIU. The arrows indicate the data flow. Green and blue waveforms indicate signals that are driving the LED in transmission or are the output of a threshold-decision after photodetection, respectively.**

PLDIU–TRX. The electrical output was then converted back to a MIL-STD-1553B differential signal and sent to a second TM (TM#2, working as RT).

The reply data from the RT followed the reverse path. The link status and the Bit Error Ratio (BER) analysis were performed by using the home-made routine described above.

B. POINT-TO-POINT TRANSMISSION

As shown in Fig. 2a, the SMU and the PLDIU are two units separated by the inner wall between room # 1 and #2; therefore, a regenerator (R1) was placed in the corresponding opening to regenerate the data. A typical sequence of packet exchanged between the two units is presented in Fig. 5. Here we report, step by step, all the waveforms of the link between the SMU and the PLDIU, from the query sent by the BC (the SMU) to the response received by RT (the PLDIU). From top to bottom, each line corresponds to signals probed at SMU, first section of R1, second section of R1 and PLDIU. The arrows indicate the logical flow of signals. We note that all waveforms reported were probed at the input of the LED transmitter or after decision-threshold and reshaping at the output of a PD: the TX signals (out) and the RX signals (in) are represented in green and blue, respectively.

In particular in Fig. 5, we can see that the communication starts when the SMU transmits optically one Command Word (CW) and two Data Words (DWs) (SMU out, green curve in the first row); following the vertical arrows, we see the signal received by the R1 and regenerated (curve in blu, in the second row), then the signal transmitted (R1.2 out, curve in green, in the third row) optically in room #2. The optical signal was then received by the PLDIU (PLDIU in, curve in blu, in the fourth row)). The PLDIU then responds by sending the Status Word (SW) (PLDIU out). Passing through the same regenerator R1 (R1.2 in and R1.1 out), the signal finally reaches the SMU (SMU in).

Each signal is the result of the reshaping operation and thus its amplitude is always about 5 V. For the sake of completeness, we report that a short delay was noticed among the signals occurs during the optical transmission (50 ns maximum), mainly due to the optical path of the signal, filtering effects and signal adaptation. Clearly, this delay cannot be observed from Fig. 5 and, moreover, it is negligible for the MIL-STD-1553B protocol, since the response time is valid within the time window of 4–12 µs [23].

The BER analysis showed that no erroneous bit was obtained in a long communication time window (30 min, corresponding to around 10^9 transmitted bits). The signals reported in Fig. 5, are, by definition, nicely squared, especially those taken at the RX end. For the sake of completeness, we also report in Fig. 6 two examples of eye diagrams taken after the TIA, before decision. They were taken at two different irradiance I_{opt}, i.e., $-24\,\mathrm{dBm/cm^2}$ and $-34\,\mathrm{dBm/cm^2}$. Even at low illumination, we can appreciate the quality of the detected OWC signal.

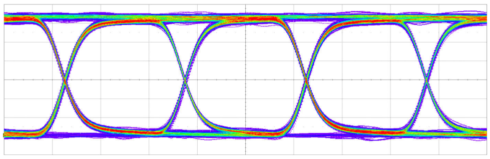

(a) $I_{opt} = -24\,\mathrm{dBm/cm^2}$; 30 mV/div; 200 ns/div

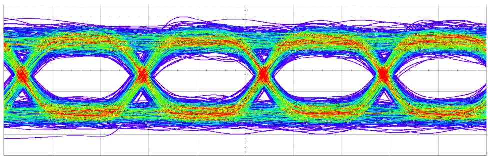

(b) $I_{opt} = -34\,\mathrm{dBm/cm^2}$; 7.5 mV/div; 200 ns/div

FIGURE 6. Eye diagrams after the TIA of an OWC transceiver, taken at two optical irradiance values representative of the high and low illumination conditions.

Similar analyses were performed for the SMU-Gyro use case. This link (see Fig. 2b) passes through three different rooms (#1 to #3) and two regenerators (R1 and R2). Also in this case, we obtained no error during transmission. The third link, between the SMU and the ST (see Fig. 2c), was the most challenging, since many units (obstacles) are present along the longer path from R1 and the ST. Notwithstanding, also in this case we do not recorded any error during the transmission.

C. BUS DEMONSTRATION

In this section, we report the complete characterization of the OWC MIL-STD-1553B bus transmission involving all the four units simultaneously. In this on-field test, the SMU sends queries to all the three RTs alternatively and each of them responds when queried. In Fig. 7, we report the output (red) and input (blue) waveforms of the SMU, where we highlighted the different messages addressed to the different RTs and the respective responses. As mentioned before, each RT responds to the BC after its own query. In this example, PLDIU responds with only the SW, the Gyro responds with the SW and, after a new request from BC, responds with two DWs; similar for ST that responds with three DWs. This shows that all the connections are working correctly (no responses if the data are not correctly received).

To fully prove that the bus is operating properly, we also report in Fig. 8 the corresponding input and output electrical waveforms of the different RTs. In gray, we report the SMU queries to the individual units. The colored waveforms (red, blue, and green) are the single responses by the units. It can be noted that each RT respond only if queried, in full compliance with MIL-STD-1553B standard.

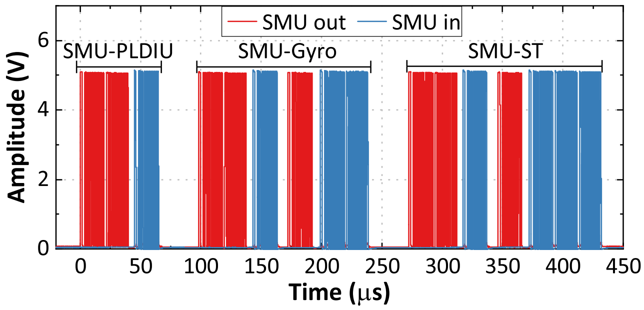

FIGURE 7. Output (red lines) and input (blue lines) waveforms by the SMU for the three links. PLDIU responded with a SW; Gyro responded with SW and 2 DWs; ST responded with SW and 3 DWs.

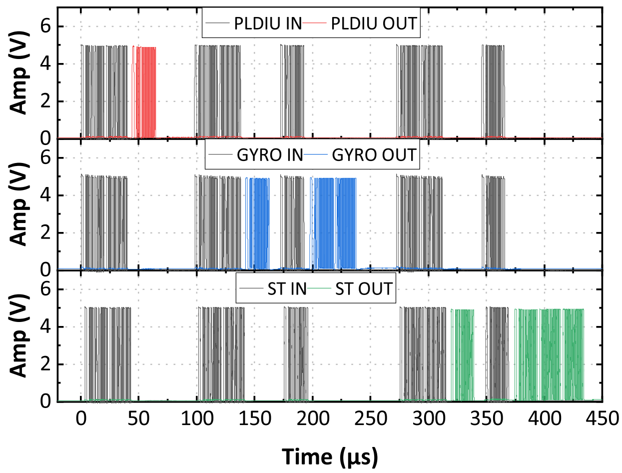

FIGURE 8. Electrical signals at the input/outputs of the RTs. top: input (gray) and output (red) signals at the PLDIU unit; middle: input and output (blue) signals at the Gyro unit; bottom: input and output (green) signals at the ST unit.

TABLE 1. Logbook of the overall MIL-STD-1553B bus links between the four units. Add: address; SA: Sub-address.

Time (µs)	Type	RT T/R	RT RX Add	RT TX Add	RT RX SA	RT TX SA	Data	Word Count	Error
0	BC-RT	R	1		10		BC10	1	
73	BC-RT	R	2		20		BC20	1	
146	RT-BC	T		2		20	2201	1	
220	BC-RT	R	3		30		BC30	1	
293	RT-BC	T		3		30	3301:3302	2	
499	BC-RT	R	1		10		BC10	1	
572	BC-RT	R	2		20		BC20	1	
645	RT-BC	T		2		20	2201	1	
719	BC-RT	R	3		30		BC30	1	
793	RT-BC	T		3		30	3301:3302	2	
1000	BC-RT	R	1		10		BC10	1	
1073	BC-RT	R	2		20		BC20	1	
1146	RT-BC	T		2		20	2201	1	
1220	BC-RT	R	3		30		BC30	1	
1293	RT-BC	T		3		30	3301:3302	2	

In Table 1, we present an extract of the long logbook of the BM (tens of millions of rows). From the left to the right column, we report the time difference between the different messages, the type of link, the direction of transmission (with respect to RT), the address and subaddress of

TABLE 2. Received optical power values in the different links (in dBm). In bold the TX-RX links actually used in the demonstration.

Rx \ Tx	SMU	PLDIU	Gyro	ST	R1.1	R1.2	R2.1	R2.2
SMU	(-19.2)				**-21.3**			
PLDIU		(-19.6)		-38.4		**-23.5**	-26.9	
Gyro			(-19.5)					**-24.4**
ST		-42.4		(-29.1)		**-34.1**	-33.6	
R1.1	**-24.7**				(-19.9)			
R1.2		**-23.9**		**-36.1**		(-25.8)	**-23.5**	
R2.1		-26.9		-37.0		**-22.2**	(-19.3)	
R2.2			**-24.7**					(-17.0)

the MIL-STD-1553B RT, the transmitted data in hexadecimal format, and the number of DWs. To easily identify the corresponding RT, we assigned address and subaddress with 1 and 10 to PLDIU, 2 and 20 to Gyro, and 3 and 30 to ST link, respectively. As an example, in the first line of Table 1 we report the transmission between BC and the PLDIU-RT; the second line shows the transmission between BC and Gyro-RT; in the third line, the Gyro responds with 1 DW to the BC. All the other lines can be read accordingly. The successful transmission is proved by the fact that the error column is empty, i.e., none of the links was reporting errors. Therefore, the complete bus MIL-STD-1553B transmission over OWC was demonstrated successfully.

IV. OPTICAL POWER CHARACTERIZATION

A. RECEIVED OPTICAL POWER VALUES

In order to have a better understanding of the links, we measured the optical power values of all the links involved in the optical communication. We used the same setup of the OWC bus demonstration, where all the links were bidirectional. For each of the TRXs, we measured the received optical power generated by the other devices in the same room. We also included the received optical power generated by the TRX itself (back reflection). As an example, in room #1, we measured the optical power received by R1 generated by the SMU and by the regenerator itself, and vice-versa. All the measured data are summarized in Table 2, between devices belonging to the same rooms.

According to these data, in all the links the received optical power value is much higher than the RX sensitivity (−37.5 dBm [26]). As aforementioned, only links between BC and RTs are realized, as the exchange of data between two RTs is always controlled by the BC, in compliance with the standard [23].

B. IRRADIANCE DISTRIBUTION

We finally performed a complete characterization of the mock-up, in order to estimate the possibility to establish effective OWC links in other positions than those reported in the previous section. To this aim, we performed a complete mapping of the optical irradiance of the inner surfaces of the mock-up, considering the main optical source in each room: SMU in room #1, R1 in room #2 and R2 in room #3. As in the previous tests, the mock-up was populated with dummy units to better emulate a real satellite. This measurement allows to estimate the communication performance when many other RTs devices are placed in different positions in the mock-up: comparing these values with the RX sensitivity (and considering the active area of the PD of ∼1 cm^2), we can quickly see if the communication is feasible or not.

To measure the intensity, we used a wide area PIN-PD (∼300 mm^2, responsivity of 0.47 A/W at 850 nm). The optical sources are the same as those used in the other tests, but now they are not modulated, with the average emitted optical power equal to the one used during the transmission analysis.

In Fig. 9, we report the irradiance measured over the inner mock-up surfaces (except the top, due to practical issues), unrolled to show them in a 2D plot. We separately present the three rooms under analysis: (a) room #1; (b) room #2; (c) room #3. In the first two figures, two small white circles indicate the position of the light source in the room (the unit positions are also present in Fig. 2). In Fig. 9c, the source is on the top surface (along the vertical line from the gray dashed circle).

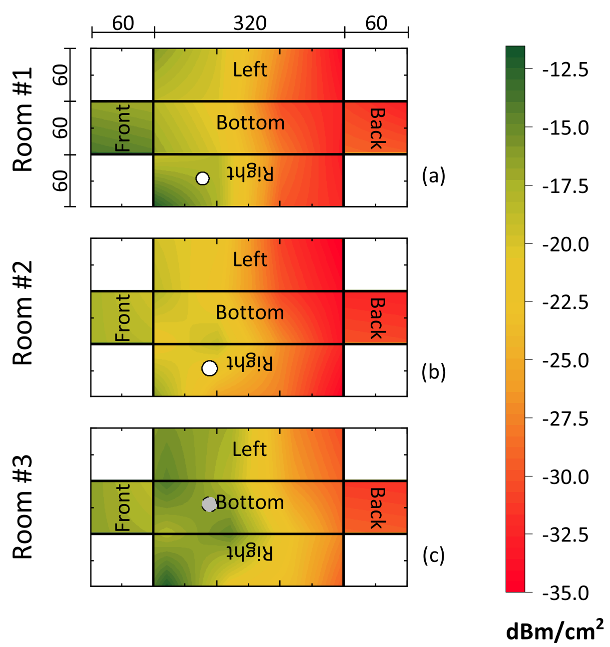

FIGURE 9. Distribution of the optical power in the three rooms over 5 of the rectangular surfaces (ceiling cannot be measured): (a) room #1; (b) room #2; (c) room #3. In each case, the light source is at the position of the white circles. Length units are in cm.

As expected, the irradiance is not uniform and we found it lower when measured far from the optical source. However, considering all cases, the lowest detected value the intensity is around -33 dBm, which is quite higher than the RX sensitivity (-37.5 dBm at BER=10^{-12}, [26]) of our TRXs. Therefore we have around 5 dB margins: this allows to safely assume that wherever the RT position is, the transmission will be feasible.

V. CONCLUSION

We reported the successful demonstration of an innovative OWC transmission of the MIL-STD-1553B signals inside a satellite. To this aim, we designed and developed new OWC boards that can be interfaced to the existing equipment, providing wireless and bidirectional communication among them. The transceivers are interchangeable among the connected units and fully preserve the backward compatibility with the existing MIL-STD-1553B bus architecture. We tested them by means of an in-field experiment, using the mockup of a real satellite and placing four transceivers in the positions of different key units. We carried out successfully the complete transmission analysis, which included four different units working simultaneously. No error was observed during the communication tests.

In order to extend the analysis, we also measured the optical intensity over different surfaces in the satellite, observing that the received intensity is always higher than the RX sensitivity; this indicates the feasibility of transmission in any position inside the mockup. Those results confirm that OWC can be effectively used to substitute the MIL-STD-1553B cables in the SC, providing full coverage of the whole volume with the required transmission performance. Present experiments confirm that the designed system is very robust. In the future, further investigations could help to determine a methodology that could be used to estimate the ultimate limits of the NLOS approach in any generic configuration.

Finally, we note that the realized system has very attracting features for future developments, yet it can be further optimized by reducing footprint, weight and power consumption of the TRXs. Once the technology will be established in terrestrial labs, it could be moved to the very challenging space environment, with its very high requirements about reliability and performance.

Another future research line will be about designing the signal adaptation stage so that it can work with other bus standards (e.g., CAN-bus) among those that are currently used onboard.

REFERENCES

[1] R. Amini, G. Aalbers, R. Hamann, W. Jongkind, and P. G. Beethuizen, "New generations of spacecraft data handling systems: Less harness, more reliability," in *Proc. 57th Int. Astron. Congr.*, Valencia, Spain, Oct. 2006, pp. 1–4.

[2] L. Gilli, G. Cossu, M. Rannello, A. Messa, and E. Ciaramella, "An optical wireless system replacing cabled connections for the data transmission in the AIT phase," in *Proc. SPIE*, vol. 11852, Jun. 2021, Art. no. 118525T.

[3] T. Ricker, "Avionics bus technology: Which bus should I get on?" in *Proc. IEEE/AIAA 36th Digit. Avionics Syst. Conf. (DASC)*, Sep. 2017, pp. 1–12.

[4] *Wireless Network Communications Overview for Space Mission Operations, CCSDS 880.0-G-3, Green Book*, Consultative Committee for Space Data Systems (CCSDS), Reston, VA, USA, May 2017, pp. 42–47.

[5] P. N. Gineste, Y. Herlem, A. Outay, and P. Pelissou, "Assessment of wireless link budget in a satellite by modelling techniques," in *Proc. ESA Workshop Aerosp. EMC*. Venice, Italy, May 2012, pp. 1–6.

[6] Z. Sun, L. Xing, and G. Xu, "Wireless RF bus design for an intra-satellite," *J. Harbin Eng. Univ.*, vol. 33, no. 7, pp. 881–886, 2012.

[7] S. Das, S. S. Das, and I. Chakrabarti, "Hardware implementation of MIL-STD-1553 protocol over OFDMA-PHY based wireless high data rate avionics systems," in *Proc. IEEE Int. Conf. Adv. Netw. Telecommun. Syst. (ANTS)*, Bengaluru, India, Nov. 2016, pp. 1–6.

[8] R. Onrubia, D. Pascual, H. Park, A. Camps, C. Rüdiger, J. Walker, and A. Monerris, "Satellite cross-talk impact analysis in airborne interferometric global navigation satellite system-reflectometry with the microwave interferometric reflectometer," *Remote Sens.*, vol. 11, no. 9, p. 1120, May 2019.

[9] M. Z. Chowdhury, M. Shahjalal, M. K. Hasan, and Y. M. Jang, "The role of optical wireless communication technologies in 5G/6G and IoT solutions: Prospects, directions, and challenges," *Appl. Sci.*, vol. 9, no. 20, p. 4367, Oct. 2019.

[10] W. Ali, G. Cossu, L. Gilli, E. Ertunc, A. Messa, A. Sturniolo, and E. Ciaramella, "10 Gbit/s OWC system for intra-data centers links," *IEEE Photon. Technol. Lett.*, vol. 31, no. 11, pp. 805–808, Jun. 1, 2019.

[11] C.-L. Tsai and Z.-F. Xu, "Line-of-sight visible light communications with InGaN-based resonant cavity LEDs," *IEEE Photon. Technol. Lett.*, vol. 25, no. 18, pp. 1793–1796, Sep. 15, 2013.

[12] I. N'doye, D. Zhang, M.-S. Alouini, and T.-M. Laleg-Kirati, "Establishing and maintaining a reliable optical wireless communication in underwater environment," *IEEE Access*, vol. 9, pp. 62519–62531, 2021.

[13] D. Wu, Z. Ghassemlooy, H. L. Minh, S. Rajbhandari, and M. A. Khalighi, "Optimisation of Lambertian order for indoor non-directed optical wireless communication," in *Proc. 1st IEEE Int. Conf. Commun. China Workshops (ICCC)*, Xiamen, China, Aug. 2012, pp. 43–48.

[14] J. Li, Y. Chen, M. Ding, F. Shu, B. Vucetic, and X. You, "A small-cell caching system in mobile cellular networks with LoS and NLoS channels," *IEEE Access*, vol. 5, pp. 1296–1305, 2017.

[15] P. K. Esubonteng and R. Rojas-Cessa, "Restore: Low-energy drone-assisted NLoS-FSO emergency communications," *IEEE Access*, vol. 10, pp. 115282–115294, 2022.

[16] I. Arruego et al., "OWLS: A ten-year history in optical wireless links for intra-satellite communications," *IEEE J. Sel. Areas Commun.*, vol. 27, no. 9, pp. 1599–1611, Dec. 2009.

[17] N. Karafolas, Z. Sodnik, J. M. P. Armengol, and I. Mckenzie, "Optical communications in space," in *Proc. Int. Conf. Opt. Netw. Design Modeling*, Brunswick, Germany, Feb. 2009, pp. 1–6.

[18] N. Karafolas, J. M. P. Armengol, and I. Mckenzie, "Introducing photonics in spacecraft engineering: ESA's strategic approach," in *Proc. IEEE Aerosp. Conf.*, Big Sky, MT, USA, Mar. 2009, pp. 1–15.

[19] A. Santamaria, F. López-Hernández, H. Guerrero, I. Arruego, and S. Rodriguez, "Wireless infra-red links for intra-satellite communications," in *Proc. Data Syst. Aerosp. (DASIA)*, vol. 532, Prague, Czech Repulbic, Jun. 2003, pp. 1–6.

[20] P. Fortescue, G. Swinerd, and J. Stark, *Spacecraft Systems Engineering*. Hoboken, NJ, USA: Wiley, 2011.

[21] D. He, X. Li, S. Chan, J. Gao, and M. Guizani, "Security analysis of a space-based wireless network," *IEEE Netw.*, vol. 33, no. 1, pp. 36–43, Jan. 2019.

[22] K. Siji and N. Saritha, "FPGA implementation of MIL-STD-1553B bus protocol controller for aircrafts," *Int. J. Sci. Res.*, vol. 4, no. 7, p. 2556, 2013.

[23] *Digital Time Division Command/Response Multiplex Data Bus*, Standard AS15531A, Department of Defense, 2018.

[24] E. Ciaramella, G. Cossu, E. Ertunc, L. Gilli, A. Messa, M. Rannello, M. Presi, A. Sturniolo, F. Bresciani, and V. Podda, "TOWS: Introducing optical wireless for satellites," in *Proc. 21st Int. Conf. Transparent Opt. Netw. (ICTON)*, Angers, France, Jul. 2019, pp. 1–4.

[25] F. Covello, F. Battazza, A. Coletta, E. Lopinto, C. Fiorentino, L. Pietranera, G. Valentini, and S. Zoffoli, "COSMO-SkyMed an existing opportunity for observing the earth," *J. Geodyn.*, vol. 49, nos. 3–4, pp. 171–180, 2010.

[26] G. Cossu, L. Gilli, E. Ertunc, and E. Ciaramella, "Transporting MIL-STD-1553 signals by means of optical wireless interfaces," *IEEE Photon. J.*, vol. 14, no. 1, pp. 1–8, Feb. 2022.

GIULIO COSSU received the M.S. degree in physics from the University of Pisa, Italy, in 2010, and the Ph.D. degree from Scuola Superiore Sant'Anna (SA), Pisa. Currently, he is an Assistant Professor with SA. The main topic of his thesis was the investigation of innovative solutions for optical wireless communications (OWC). He was a Scientific Responsible/Technical Officer with SA for the project "High Throughput Optical Network (HYDRON)" and "HYDRON Simulation TestBed," both funded by the European Space Agency (ESA). He was in the workgroup about the development of optical wireless links for intra/extra spacecraft and AIT scenarios within the framework of the TOWS project founded by ESA. He is the author or coauthor of about 70 publications and holds four international patents. His research interests include optical propagation through the atmosphere, optical characterization, and optical communications.

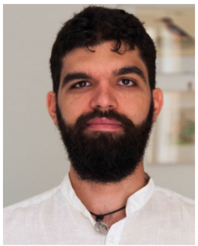

LORENZO GILLI was born in Rome, in 1989. He received the M.S. degree in physics from Roma Tre University, Rome, Italy, in December 2016. He is currently pursuing the Ph.D. degree with Scuola Superiore Sant'Anna, Pisa, with a research project on optical wireless communication (OWC). Here, he worked on visible light communication (VLC) systems for indoor positioning and OWC systems for space applications. During his course of study, he collaborated with the Italian National Institute for Geophysics and Volcanology (INGV) to study ionospheric and atmospheric dynamics.

NICOLA VINCENTI received the degree in electronic engineering theory from the University of Pisa, in December 2002, the master's degree in microelectronic designs from the Physics Department, University of Padua, Italy, in 2006. Since then, he has contributed to developing and deploying many test programs for electronic device verification and validation with few test engineering societies working in the context of Teradyne Test Equipment facilities. He is currently with the OWC Laboratories, Scuola Superiore Sant'Anna, Pisa, Italy, for the design and improvement of systems on the treatment and transduction of optical signals to electrical analysis and transmission to digital interfaces.

EMILIANO PIFFERI received the degree in electronic engineering from the Sapienza University of Rome, Italy. At Thales Alenia Space Italia S.p.A., Roma, Italy, he is currently the Head of the Harness Engineer Department, TAS-I, where is responsible for all the projects with respect to harness design in LEO, MEO, GEO, and telecommunication satellites. He has been managing and coordinating several projects for the European Space Agency, European Commission, and others. In addition, he is collaborating mainly with the development of optical technologies for space applications for reducing harness time in integration and weight.

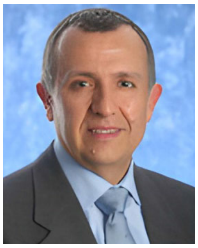

VINCENZO SCHENA received the degree in physics from the University of Bari, Italy, and the Ph.D. degree in mathematic models for engineering from the Sapienza University of Rome, Italy. Formally, he is a Satellite Communication Systems Expert and a certified INCOSE System Engineer Professional (CSEP). At Thales Alenia Space Italia S.p.A., Roma, Italy, he is currently the Head of research and development at Domain Telecommunication Italy, where he is managing and coordinating several projects and studies towards international entities as the European Space Agency, the European Commission, and others. In addition, he is collaborating mainly with the development of optical technologies for space applications and the 5G NTN Protocol for future space network systems covering all the systems and technical aspects.

ERNESTO CIARAMELLA (Senior Member, IEEE) joined as an Associate Professor with Scuola Superiore Sant'Anna, Pisa, in 2002, where he has been a Full Professor of telecommunications with Istituto TeCIP, since 2014. He is the author or coauthor of about 250 publications and holds 25 international patents. He participated in several European research projects. He has been coordinator of the EU-FP7 Project COCONUT, from 2012 to 2015. He is currently a principal investigator of the ESA-TOWS project about optical wireless systems. His research interest includes optical communications (components, systems, and networks). His main research contributions are related to devices for the regeneration of the optical signal, the design of WDM systems for transport networks and access, and free-space optical systems (optical wireless).

Open Access funding provided by 'Scuola Superiore "S.Anna" di Studi Universitari e di Perfezionamento' within the CRUI CARE Agreement